coatings | MDPI

Effect of SiO$_2$ Sol/Silane Emulsion in Reducing Water and Chloride Ion Penetration in Concrete

Yongjuan Geng [1,2]**, Shaochun Li** [1,2,*]**, Dongshuai Hou** [1,2]**, Xu Chen** [3] **and Zuquan Jin** [1,2]

1   School of Civil Engineering, Qingdao University of Technology, Qingdao 266033, China;
    gengyongjuan@qut.edu.cn (Y.G.); houdongshuai@qut.edu.cn (D.H.); jinzuquan@qut.edu.cn (Z.J.)
2   Engineering Research Center of Concrete Technology under Marine Environment, Ministry of Education,
    Qingdao University of Technology, Qingdao 266033, China
3   China West Construction Group Xinjiang Co., Ltd., Urumqi 830000, China; chenxu@qut.edu.cn
*   Correspondence: lishaochun@qut.edu.cn

check for updates

Abstract: Here, a new concrete hydrophobic treatment method is developed using SiO$_2$ sol and silane emulsion. The effectiveness of the modification for concrete protection is evaluated through testing water absorption and chloride diffusion. Two types of concrete with different strength grades (C40, C50) are used as the research object. The results show that the water capillary absorption coefficient and chloride ion diffusion coefficient of concrete decrease greatly under the protection of SiO$_2$ sol and silane emulsion. Additionally, the protection effect is better with the increase of SiO$_2$ consumption. Contact angle test results reveal that when the coating amount of SiO$_2$ sol and silane emulsion is 300 g/m^2, respectively, the contact angle reaches 150.2°, indicating the concrete (C40) surface reaches the superhydrophobic state. Through scanning electron microscope (SEM) observation, it is found that the hydrophobic effect of the SiO$_2$ sol/silane emulsion is mainly due to the change in the surface morphology of concrete (C40).

Keywords: concrete; hydrophobic; water capillary absorption; chloride ion diffusion; contact angle

1. Introduction

Concrete is a porous material with a large amount of pores and micro cracks on its surface, allowing water to penetrate into the concrete easily due to the capillary forces. Although there are many factors that can lead to concrete damage, water transport properties are still the direct factor leading to the decline of concrete durability [1]. Accordingly, chloride, sulphate, and other soluble aggressive agents can be absorbed by concrete, and their reaction with oxygen can rust the steel bars to cause the cracking of concrete [2–5]. The corrosion will propagate further, which results in structure failure which influences the durability of the structure. Therefore, if certain measures are not taken, it is inevitable that water will enter the concrete and cause corrosion.

Although many studies have been conducted on the evaluation of the waterproof performance of concrete, there is a necessity for more attention in this area. Previously, various strategies were used to protect concrete from water penetration [6–8]. Nowadays, several chemicals on the market are being applied to extend the service life of concrete structures. The impregnating agents (water repellents, hydrophobic agents) such as silane are a kind of very effective material to protect concrete from water penetration [9]. Silane can penetrate into concrete for a certain depth and interact with hydrated cement particles to form a water repellent layer which can repel water without sealing the pores of the concrete [10–12]. Thus, impregnating agents have almost the same service life as normal concrete.

Recently, the effect of silane-based impregnating agent treatments on concrete surfaces has been evaluated by testing water absorption [13–15], chloride ion diffusion [16–18], carbonation depth [19,20],

and freeze–thaw resistance [21,22]. Many study results have proven that silane can reduce the diffusion of water and chloride ions, inhibit carbonation, increase frost resistance, and delay the corrosion rate of steel reinforcements. A summary on the effect of silane-based impregnating agents on the corrosion of concrete was provided by Pan et al. [23,24]. However, even if silanes have proven to be more suitable and are widely applied in concrete structures nowadays, there is still a need to further enhance their barrier properties and to improve their waterproof efficacy in typical service environments.

Concurrently, as a nanometer-scale material, SiO_2 sol has a pozzolanic reactivity effect in Portland cement [25–27]. Therefore, it is expected to improve the compactness of the concrete surface and reduce water absorption. Liu et al. [28] studied the effects of colloidal nano-SiO_2 (CNS) on the immobilization of chloride ions in the cement-fly ash system. They reported that CNS refined the pore structure of the cement and improved the immobilized chloride ratio. Kumar et al. [29] investigated the effect of nano-SiO_2 (NS) on the durability properties of cement mortar. The results showed that substituting NS up to 2% can improve the strength, durability, and microstructure of mortar specimens, which results in better performance than the conventional one.

Recently, researchers have found that a superhydrophobic surface can be obtained using silane and NS together [30,31]. However, there are few reports on the realization of a superhydrophobic effect on a concrete surface. Here, we try to form a superhydrophobic layer on a concrete surface by applying SiO_2 sol and a silane emulsion. Water capillary absorption and the chloride ion penetration coefficient are measured and their dependence on the SiO_2 sol amount is established. Additionally, the surface morphology is examined using SEM. These measured quantities are additional parameters necessary to be considered for the optimal protection of a concrete structure used in a marine environment.

2. Materials and Methods

2.1. Materials

2.1.1. Concrete

Cement used in this experiment is a commercial Portland cement type P.O. 42.5. The proportion of the concrete used in this study is shown in Table 1. Natural sand with a 2 mm maximum size and gravel with a 25 mm maximum size were used as fine and coarse aggregates, respectively. The concrete specimens were prepared using 100 mm × 100 mm × 100 mm molds (for the capillary water absorption test and the capillary chloride salt suction experiment) and 100 mm × 300 mm^2 molds (for the chloride ion permeability coefficient test). The samples were demolded after 24 h of curing, then they were placed in a curing room (20 ± 2 °C, relative humidity (RH) ≥ 90%) for 14 days. After 14 days, the samples were cut into two halves. Subsequently, these half cubes were placed in the humid room until they were 28 days. The compressive strength of the concrete with 100 mm × 100 mm × 100 mm after 28 days curing is shown in Table 1.

Table 1. Concrete composition [$kg \cdot m^{-3}$].

Strength Grade	Cement	Sand	Gravel	Water	Superplasticizer	Water Cement Ratio (W/C)	Compressive Strength (MPa)
C50	380.0	579.0	1269.0	152.0	1%	0.4	52.6
C40	320.0	653.0	1267.0	160.0	0.8%	0.5	44.7

2.1.2. Preparation of Triethoxy(Isobutyl)Silane Emulsion and SiO_2 Sol

Triethoxy(isobutyl)silane monomers were selected to synthesize the silane emulsion. Deionized water was used as the solvent. Span 80 (100% purity) and Peregal-O (100% purity) were used as the emulsifier. Polyethylene glycol 2000 (PEG2000) was used as the stabilizer. The synthesizing procedure was as follows: (i) a certain amount of monomer and emulsifier were added to a round-bottom flask; (ii) an aqueous solution of PEG2000 (50% concentration) was added into the flask over a magnetic

stirrer maintained at 55 °C, and the mixture was stirred at the speed of 2000 r min^{-1}; (iii) a silane emulsion was obtained after 7 h of reaction followed by cooling.

SiO$_2$ sol was prepared as normal from tetraethyl orthosilicate (TEOS, 100% purity), ethanol (EtOH, 99.5% purity), H$_2$O and HNO$_3$ (65% purity). First, TEOS and EtOH were mixed with a molar ratio of 1:1, and stirred at room temperature for 10 min. Second, 0.1 M HNO$_3$ in water was added dropwise to the solution until the H$_2$O and TEOS molar ratio of 4:1 was attained. Finally, the solution was then stirred at 50 °C for 2 h to obtain SiO$_2$ sol.

Table 2 shows the characteristic of the silane emulsion and SiO$_2$ sol. The pH value was measured by a pH-meter (PHS-3C, INESA, Shanghai, China). The viscosity of the silane emulsion and SiO$_2$ sol were measured using a viscosity meter (DV-S, Brookfield, Middleboro, MA, USA).

Table 2. Characteristic of silane emulsion and SiO$_2$ sol.

Form	Appearance	pH Value	Stability	Silane Content	Viscosity (mPa·s)	Note
Isobutyl-triethoxy silane emulsion	Milk white, no precipitation	7.2	>6 months	50.5%	5.1	Available water dilution, silane emulsion
SiO$_2$ sol	transparent, yellowish, no precipitation	6.0	>12 months	–	5.5	Available water dilution, SiO$_2$ sol

2.2. Formation of Hydrophobic Layer on Concrete Surface

Concrete specimens were dried in an oven at 60 °C for 48 h after being removed from the curing room. The surfaces of the specimens were polished and cleaned. The lateral side of the concrete specimens were sealed with epoxy resin, leaving the two opposite surfaces as coating-hydrophobic layers. First, SiO$_2$ sol was applied in different amounts (Table 3) carefully using a brush on the surfaces of the specimens. Second, a silane emulsion was coated on the surface of the specimens after 3 h, and repeated two times, 6 h apart. Finally, the specimens were put aside in ambient conditions for 7 days before carrying out the tests.

Table 3. Consumption of SiO$_2$ sol and silane emulsion on concrete surface (g/m^2).

| Type	SiO$_2$ Sol	Silane Emulsion
S0	0	600
S1	100	500
S2	200	400
S3	300	300

2.3. Test Process and Method

2.3.1. Capillary Water Absorption

To evaluate the effectiveness of the hydrophobic layer, a capillary water absorption test was carried out according to standard UNI EN 1015-18:2004 (Figure 1a) [32]. Figure 1b shows concrete specimens were placed in a pan where they were immersed in deionized water at a depth of 3–6 mm above the exposed surface, at room temperature. The pan was covered to prevent water evaporation. The amount of absorbed water over time was measured by weighing the samples after 1, 2, 4, 6, 8, 12, 24, and 36 h. The water capillary coefficient typically fits the following equation [33]:

$$A = \frac{\Delta W}{\sqrt{t}} \tag{1}$$

where A is the coefficient (g·m^{-2}·h$^{-0.5}$), ΔW is the mass of water absorbed per unit exposed area (g·m^{-2}), t is the time (h).

(a)   (b)
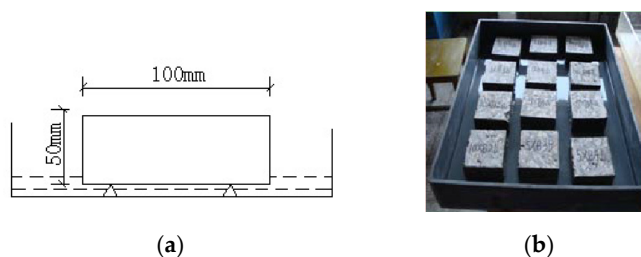
Figure 1. (**a**) Schematic of concrete capillary absorption test; (**b**) Concrete capillary absorption test.

Water capillary sorption tests were carried out on three replicates of each sample.

2.3.2. Chloride Penetration

The procedure for the chloride penetration test was similar to that for the water absorption test, except that the water was replaced by a 3% NaCl solution. During the soaking test, the container was covered to prevent the change in density caused by evaporation. After soaking, the specimens were dried at 105 ± 5 °C. The chloride content of the concrete was analyzed using the Volhard Titration Method (BS EN 12469 (2007) [34]). The concrete powder was collected by a mill. The chloride content was reported as wt.% by cement weight. The chloride content values were averaged among the values obtained by the analyses carried out on three specimens of each concrete type.

2.3.3. Chloride Diffusion Coefficients

The chloride diffusion coefficient test was conducted in accordance to the procedure of the rapid chloride migration (RCM) method described by Luping Tang. Concrete slices of 50 mm in thickness were obtained by sawing the cylindrical specimen (100 mm × 300 mm^2). The slices were kept in an oven at 105 ± 5 °C until obtaining a constant mass. Then, the hydrophobic layer was applied to the circular surfaces of the specimens. After seven days, the specimens were saturated using the procedure of ASTM C 1202-97 [35]. The slice was placed between two cells. One cell was filled with a 0.3 mol L^{-1} NaOH solution and the other with a 10.0% NaCl solution. The cells were connected to a 30 V power source. The temperature of the test specimens and solution was 20–25 °C. The penetration depth of the chloride ions into the concrete was measured based on the depth of the colour change of a surface of concrete broken in the direction of the chloride flow using a 0.1 M AgNO$_3$ solution.

2.3.4. Contact Angle Measurement

To evaluate the hydrophobic layer properties on concrete, the contact angle measurements were performed using an OCA-20 Contact Angle Instrument (Data Physics Instruments, Inc., Filderstadt, Germany). The optical system of the device adopts a digital CMOS camera. Water drops, with the size of about 5 μL, were placed at five different points on the specimen surface and the contact angle was measured immediately (Figure 2). The reported contact angle values were averages of five measurements conducted for each test. During the test, an automatic ring fitting method was used to calculate the contact angle.

| (**a**) | (**b**) |
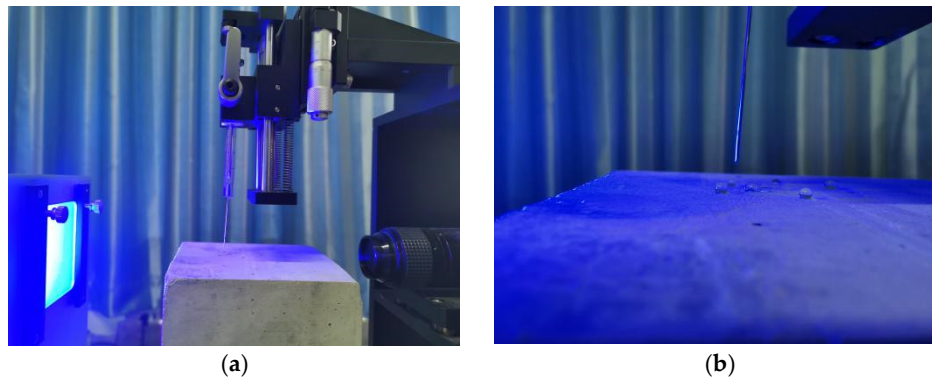
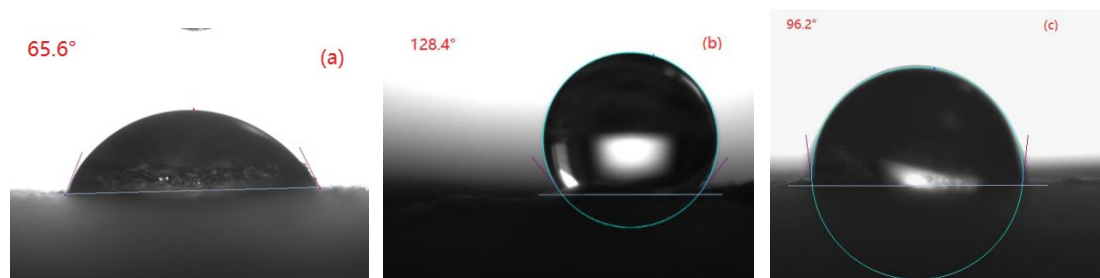**Figure 2.** Contact angle test of the concrete: (**a**) test device; (**b**) test process.

2.3.5. SEM

The morphologies of the treated concrete surfaces by hydrophobic layer, prepared in this study, were investigated using SEM (S3500N, HITACH, Tokyo, Japan). SEM test samples were taken from the concrete surface to a 4 mm depth using a cutting method.

3. Results and Discussion

3.1. Effect of SiO$_2$ Sol/Silane Emulsion on Water Contact Angle on Concrete

During the contact angle test, C40 concrete samples were taken as the test object. The main reason is that the porosity of C40 concrete is larger than that of C50 concrete, thus it more easily absorbs water. When a superhydrophobic structure can be constructed on the surface of a C40 concrete, it will be more practical. Figure 3a shows the contact angle of the untreated concrete. We can see that the water drop spread on the concrete surface and the contact angle values were just 65.6°. It is believed that concrete is a hydrophilic material. When water contacts with concrete, it can penetrate into the concrete surface by means of capillary forces spontaneously.

Figure 3. Contact angle of the concrete surface: (**a**) untreated; (**b**) treated by silane emulsion; (**c**) treated by SiO$_2$.

When the silane emulsion was used on the concrete surface, the concrete achieved hydrophobicity. Figure 3b shows the images of water droplets on the concrete surface treated with silane emulsion, as well as the value of the contact angle. It was found that the contact angle increased by more than 95%, to achieve 128.4°. Moreover, when the SiO_2 sol was applied onto the concrete surface only, the contact angle increased slightly to 96.2° compared with the untreated surface (Figure 3c). This shows that the hydrophobic effect of concrete is not good if SiO_2 sol is used alone.

The contact angles for the concrete surfaces treated by the SiO_2 sol/silane emulsion with different SiO_2 sol amounts are given in Figure 4a–c. It can be seen that, with the use of SiO_2 sol, the contact angle of the concrete surface was enhanced to about 140°. Moreover, with the growing amount of SiO_2 sol, the contact angle increased constantly. Moreover, the Figures show when the 100 g/m^2 SiO_2 sol was used on the concrete surface, the contact angle was 133.76°. When the SiO_2 sol amount increased to 300 g/m^2, however, the superhydrophobic surface was obtained because the contact angle achieved was about 150.2°.

Figure 4. Contact angle of the concrete surface treated by SiO_2 sol and silane emulsion: (**a**) S1; (**b**) S2; (**c**) S3.

Regarding the Cassie–Baxter regime mentioned previously [36], a two-length-scale, micro- and nano-hierarchical surface roughness, and a hydrophobic surface are important to achieve super-hydrophobicity. Here, the super-hydrophobic effect was the consequence of the combination of the SiO_2 sol, which introduced the micro- and nano- roughness, and the silane emulsion, which provided the hydrophobic surface on the concrete. Concurrently, it should be noted that the SiO_2 sol/silane emulsion is not considered a type of paint, but an impregnation agent.
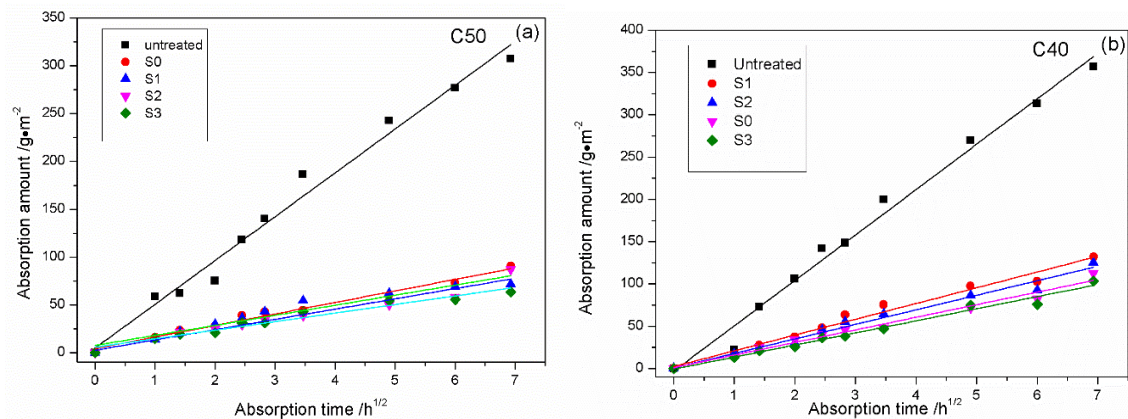
3.2. Effect of SiO_2 Sol/Silane Emulsion on Water Absorption in Concrete

The decrease in water uptake of concrete surfaces can be a criterion for the evaluation of the efficacy of the hydrophobic treatment. To verify if the SiO_2 sol/silane emulsion layers could improve the resistance of the treated concrete to the penetration of water, capillary absorption tests were performed. Figure 5a,b shows the results of water capillary absorption tests obtained for concrete specimens of C50 and C40, respectively. The curves demonstrate that the application of SiO_2 sol/silane emulsion produced a drastic decrease in the capillary absorption values compared to the untreated samples. To compare, the treatment with the SiO_2 sol/silane emulsion was more efficient than silane emulsion alone.

Table 4 presents the results of the capillary water absorption coefficients, which is the weight of water that penetrates in concrete per unit of area and time. The water absorption coefficients of the untreated concrete specimens of C50 and C40 at 24 h was 45.83 g·m^{-2}·h$^{-0.5}$ and 53.71 g·m^{-2}·h$^{-0.5}$, respectively. When the silane emulsion was coated on the concrete, the water absorption coefficients reduced by about 70%. However, the most effective treatments were those based on the SiO_2 sol/silane emulsion layer, which reduced the water absorption amount by more than 75% compared to the control. The superiority of the SiO_2 sol/silane emulsion is believed to be the result of the rise in the contact

angle between the water and the concrete surface. These changes are coherent with the contact angle data discussed above.

Figure 5. Effect of SiO_2 sol/silane emulsion with different programs on water absorption amount in concrete: (**a**) C50; (**b**) C40.

Table 4. The capillary water absorption coefficients of concrete [$g.m^{-2}\ h^{-0.5}$].

Type	C50	C40
untreated	45.83	53.71
S0	12.06	18.64
S1	10.53	17.20
S2	10.75	14.89
S3	8.95	14.31

It should be pointed out that the enhancement of the protection efficiency depends on the amount of SiO_2 sol coated on the concrete surface. Initially (S0), silane emulsion forms a thin protective film on the surface. The addition of SiO_2 sol (S1, S2, S3) leads to the formation of superficial nano-sized protrusions caused by the reaction of SiO_2 and $Ca(OH)_2$ on the concrete surface [37]. Using the 300 g/m^2 of SiO_2 sol, the SiO_2 sol/silane emulsion offers sufficient protection for concrete.
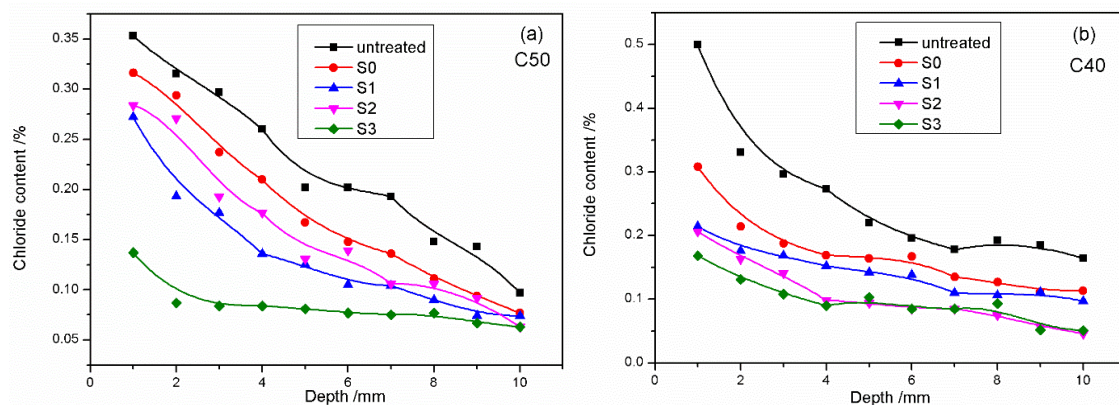
3.3. Effect of SiO_2 Sol/Silane Emulsion on Chloride Ion Diffusion in Concrete

It is believed that the water capillary action during the transport is the fundamental role of Chloride ions entering into the concrete, especially near the unsaturated concrete surface. To understand the influence of the concrete strength grade on the protection efficacy of the SiO_2 sol/silane emulsion on preventing chloride ion penetration, C40 and C50 concrete were used. Figure 6a,b shows chloride profiles in the various depth ranges of C40 and C50, respectively. Considering the Figures, it is observed that both silane emulsion and SiO_2 sol/silane emulsion can reduce deep chloride ion penetration relative to the control sample. Similar to the capillary water absorption test, SiO_2 sol/silane emulsion performs better than silane emulsion. Regarding a 6 mm depth in C40 concrete, for example, SiO_2 sol/silane emulsion gives an approximately 29.6%–56.6% reduction in chloride ion concentration, while silane emulsion gives approximately 14.8%.

Moreover, chloride ion content was decreased gradually with the increased coating amount of SiO_2 sol. The observed effect also can be explained by changes in the surface contact angle of the treated concrete caused by the addition of SiO_2 sol.

Table 5 presents the results of chloride ion penetration depth and diffusion coefficients determined using the RCM method. The results indicate that the application of silane emulsion and SiO_2 sol/silane emulsion on the concrete surface causes the reduction of the chloride ion penetration depth and diffusion coefficient. Regarding C50 concrete treated with a SiO_2 sol/silane emulsion, the chloride diffusion

coefficient, ranged only by $1.4–1.1 \times 10^{-12}$ m$^2 \cdot$s^{-1}, is about one-tenth of that of the concrete without treatment. Concurrently, the penetration depth of the chloride ions is reduced about 64.1%–57.5%.

Figure 6. Effect of SiO$_2$ sol/silane emulsion with different programs on chloride profiles in concrete: (**a**) C50; (**b**) C40.

Table 5. Effect of SiO$_2$ sol/silane emulsion with different programs on chloride penetration and diffusion coefficients.

| W/C	Chloride Diffusion Coefficient/(10^{-12} m$^2 \cdot$s^{-1})					Penetration Depth/mm				
	Untreated	S0	S1	S2	S3	Untreated	S0	S1	S2	S3
C50	9.2	1.6	1.4	1.1	1.1	17.35	8.32	7.38	6.47	6.23
C40	10.4	1.8	1.7	1.5	1.2	18.46	10.52	8.21	7.72	6.57

However, when concrete with a lower strength grade is used, the surface treatment seems more effective in reducing chloride penetration. Particularly, the concrete with a SiO$_2$ sol/silane emulsion treatment is always able to reduce the chloride diffusion coefficient significantly by at least 83.7% when C40 concrete is used.

It should be noted that this type of result is only related to the penetration of chloride ions by diffusion (saturated concrete), excluding chloride penetration by absorption of contaminated water. Therefore, the SiO$_2$ sol/silane emulsion treatment does not primarily inhibit chloride ion penetration. The main effect is to reduce the water penetration, which may be contaminated with chloride ions. It is important to verify again that the SiO$_2$ sol/silane emulsion presented efficiency greater than the silane emulsion.

3.4. Microstructure Analysis

To analyze the changes of the concrete surface morphology, untreated and treated concrete samples using silane emulsion and SiO$_2$ sol/silane emulsion were examined using SEM. Figure 7a shows the SEM image of the untreated concrete sample surface, which is rough and some pores or cracks are present. Figure 7b is the SEM image of the concrete surface treated by silane emulsion. The image clearly shows that the silane emulsion does not significantly modify the substrate morphology, as expected. However, there was a remarkable change in the surface morphology of the concrete treated by the SiO$_2$ sol/silane emulsion (Figure 7c). The pre-treated by SiO$_2$ sol on concrete surface improves their pore coverage ability since the nano-SiO$_2$ tend to fill in the pores in a concrete surface [38,39]. Moreover, SiO$_2$ sol can react with the hydration product Ca(OH)$_2$ to form a secondary hydration C–S–H gel, further increasing the density of the concrete surface [40,41]. Consequently, the pore size and number for absorption or permeation of water into the concrete are effectively reduced compared to the concrete treated with the silane emulsion only. This verified that the treatment with a SiO$_2$ sol/silane emulsion has a higher protective effectiveness than silane emulsion alone.
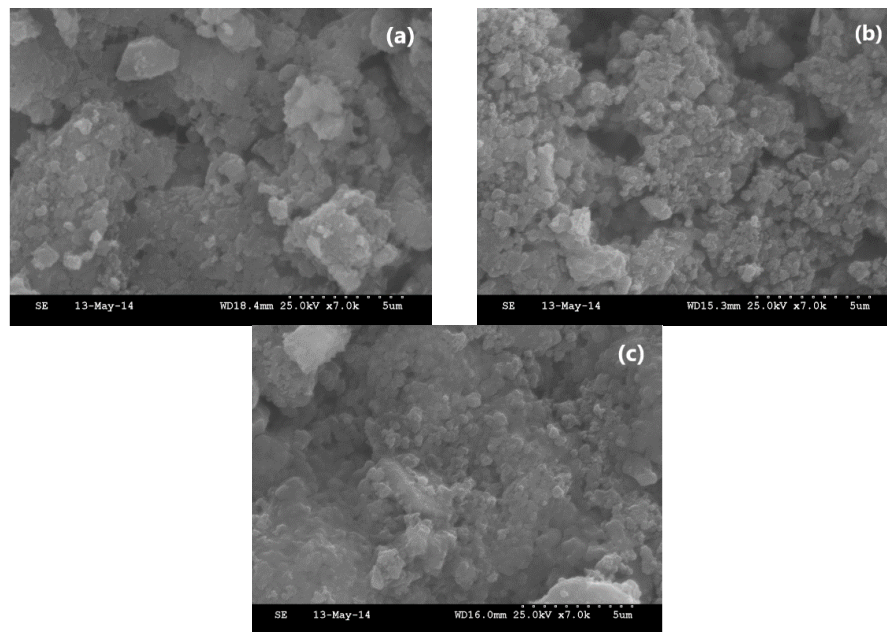
Figure 7. Micromorphology of the concrete surface treated by different materials: (**a**) without treatment; (**b**) silane emulsion; (**c**) SiO_2 sol/silane emulsion (S3).

Figure 8 shows the results of an energy dispersive spectrometer (EDS) test of the concrete treated by SiO_2 sol/silane emulsion (S3). Figure 8 shows that the contents of the Si and C elements are greatly increased. Among them, the C element mainly comes from carbon in silane. Table 6 provides the test results of spot scanning and surface scanning during EDS analysis. Considering the table we can see that, when the concrete (C40) was treated with SiO_2 sol only, the silicon content increased by 81.7% compared to that of the untreated concrete but, when the SiO_2 sol/silane emulsion (S3) was used, the silicon content increased by 249.5%. Similarly, the content of silicon on the concrete surface also was greatly improved in the results of the surface scanning test, indicating that the SiO_2 sol/silane emulsion (S3) could be distributed evenly on the concrete surface.
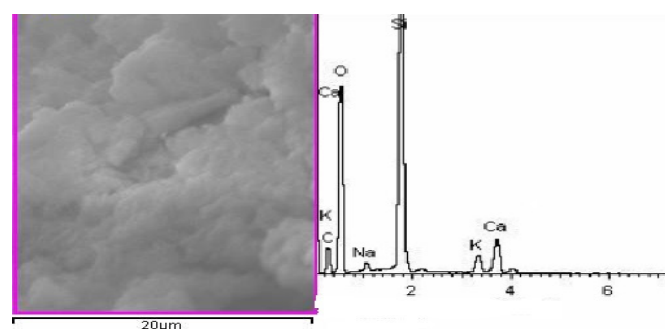
Figure 8. EDS results of the concrete surface treated by SiO_2 sol/silane emulsion (S3).

Table 6. Spot scanning and surface scanning test results in EDS analysis.

Sample	Content of Si (%)	
	Spot Scanning	Surface Scanning
Without Treatment	4.04	4.81
Treated By SiO_2 Sol	7.34	7.21
Treated By SiO_2 Sol/Silane Emulsion (S3)	14.12	10.23

4. Conclusions

A new method of concrete surface hydrophobic treatment was prepared using SiO_2 sol and silane emulsion. The consumption of SiO_2 sol is essential for the hydrophobization of the treated concrete surfaces. Regarding the case of an appropriate coating amount (SiO_2 sol and silane emulsion is 300 g/m^2, respectively), with application using the same methodology, the superhydrophobic effect was achieved and the water contact angle reached 150.2°. Concerning concrete of either C50 or C40, the water capillary absorption coefficient was reduced by 80.5% and 73.4% at most, respectively. Therefore, the combination of SiO_2 sol and silane emulsion can reduce the water capillary absorption of concrete effectively. Due to the decrease in water absorption, it is difficult for chloride ions to diffuse into the concrete. The chloride ion diffusion coefficient of concrete of either C50 or C40 was only 1.1×10^{-12} m^2·s^{-1} and 1.2×10^{-12} m^2·s^{-1}, respectively. The excellent hydrophobic effect mainly comes from the improvement of the microstructure of the concrete surface.

References

1. Dareyni, M.; Moghaddam, A.M.; Delarami, A. Effect of cationic asphalt emulsion as an admixture on transport properties of roller-compacted concrete. *Constr. Build. Mater.* **2018**, *163*, 724–733. [CrossRef]

2. Wasim, M.; Ngo, T.D.; Abid, M. Investigation of long-term corrosion resistance of reinforced concrete structures constructed with various types of concretes in marine and various climate environments. *Constr. Build. Mater.* **2020**, *237*, 117701. [CrossRef]

3. Chang, H.; Jin, Z.; Zhao, T.; Wang, B.; Li, Z.; Liu, J. Capillary suction induced water absorption and chloride transport in non-saturated concrete: The influence of humidity, mineral admixtures and sulfate ions. *Constr. Build. Mater.* **2020**, *236*, 117581. [CrossRef]

4. Rossi, E.; Polder, R.; Copuroglu, O.; Nijland, T.; Šavija, B. The influence of defects at the steel/concrete interface for chloride-induced pitting corrosion of naturally-deteriorated 20-years-old specimens studied through X-ray computed tomography. *Constr. Build. Mater.* **2020**, *235*, 117474. [CrossRef]

5. Balestra, C.E.T.; Nakano, A.Y.; Savaris, G.; Medeiros-Junior, R.A. Reinforcement corrosion risk of marine concrete structures evaluated through electrical resistivity: Proposal of parameters based on field structures. *Ocean Eng.* **2019**, *187*, 106167. [CrossRef]

6. Li, G.; Yue, J.; Guo, C.; Ji, Y. Influences of modified nanoparticles on hydrophobicity of concrete with organic film coating. *Constr. Build. Mater.* **2018**, *169*, 1–7. [CrossRef]

7. Wang, Q.; Li, S.; Pan, S.; Guo, Z. Synthesis and properties of a silane and copolymer-modified graphene oxide for use as a water-reducing agent in cement pastes. *New Carbon Mater.* **2018**, *33*, 131–139. [CrossRef]

8. Cai, Y.; Hou, P.; Duan, C.; Zhang, R.; Zhou, Z.; Cheng, X.; Shah, S. The use of tetraethyl orthosilicate silane (TEOS) for surface-treatment of hardened cement-based materials: A comparison study with normal treatment agents. *Constr. Build. Mater.* **2016**, *117*, 144–151. [CrossRef]

9. Herb, H.; Gerdes, A.; Brenner-Weiß, G. Characterization of silane-based hydrophobic admixtures in concrete using TOF-MS. *Cement Concr. Res.* **2015**, *70*, 77–82. [CrossRef]

10. Shea, W.; Du, Y.; Miao, C.; Liu, J.; Zhao, G.; Jiang, J.; Zhang, Y. Application of organic- and nanoparticle-modified foams in foamed concrete: Reinforcement and stabilization mechanisms. *Cement Concr. Res.* **2018**, *106*, 12–22. [CrossRef]

11. Shen, L.; Jiang, H.; Wang, T.; Chen, K.; Zhang, H. Performance of silane-based surface treatments for protecting degraded historic concrete. *Prog. Org. Coat.* **2019**, *129*, 209–216. [CrossRef]

12. Zhu, Y.-G.; Kou, S.-C.; Poon, C.-S.; Dai, J.-G.; Li, Q.-Y. Influence of silane-based water repellent on the durability properties of recycled aggregate concrete. *Cem. Concr. Compos.* **2013**, *35*, 32–38. [CrossRef]

13. Sudbrink, B.; Moradllo, M.K.; Hu, Q.; Ley, M.T.; Davis, J.M.; Materer, N.; Apblett, A. Imaging the presence of silane coatings in concrete with micro X-ray fluorescence. *Cem. Concr. Res.* **2017**, *92*, 121–127. [CrossRef]

14. Moradllo, M.K.; Sudbrink, B.; Ley, M.T. Determining the effective service life of silane treatments in concrete bridge decks. *Constr. Build. Mater.* **2016**, *116*, 121–127. [CrossRef]

15. Christodoulou, C.; Goodier, C.I.; Austin, S.A.; Webb, J.; Glass, G.K. Long-term performance of surface impregnation of reinforced concrete structures with silane. *Constr. Build. Mater.* **2013**, *48*, 708–716. [CrossRef]

16. Xue, X.; Li, Y.; Yang, Z.; He, Z.; Dai, J.-G.; Xu, L.; Zhang, W. A systematic investigation of the waterproofing performance and chloride resistance of a self-developed waterborne silane-based hydrophobic agent for mortar and concrete. *Constr. Build. Mater.* **2017**, *155*, 939–946. [CrossRef]

17. Petcherdchoo, A.; Chindaprasirt, P. Exponentially aging functions coupled with time-dependent chloride transport model for predicting service life of surface-treated concrete in tidal zone. *Cem. Concr. Res.* **2019**, *120*, 1–12. [CrossRef]

18. Liu, J.; Cai, J.; Shi, L.; Liu, J.; Zhou, X.; Mu, S.; Hong, J. The inhibition behavior of a water-soluble silane for reinforcing steel in 3.5% NaCl saturated $Ca(OH)_2$ solution. *Constr. Build. Mater.* **2018**, *189*, 95–101. [CrossRef]

19. Aguiar, J.B.; Júnior, C. Carbonation of surface protected concrete. *Constr. Build. Mater.* **2013**, *49*, 478–483. [CrossRef]

20. Tittarelli, F.; Moriconi, G. The effect of silane-based hydrophobic admixture on corrosion of reinforcing steel in concrete. *Cem. Concr. Res.* **2008**, *38*, 1354–1357. [CrossRef]

21. Guo, T.; Weng, X. Evaluation of the freeze-thaw durability of surface-treated airport pavement concrete under adverse conditions. *Constr. Build. Mater.* **2019**, *206*, 519–530. [CrossRef]

22. Karthick, S.; Park, D.-J.; Lee, Y.S.; Saraswathy, V.; Lee, H.-S.; Jang, H.-O.; Choi, H.-J. Development of water-repellent cement mortar using silane enriched with nanomaterials. *Prog. Org. Coat.* **2018**, *125*, 48–60. [CrossRef]

23. Pan, X.; Shi, Z.; Shi, C.; Ling, T.-C.; Li, N. A review on concrete surface treatment part I: Types and mechanisms. *Constr. Build. Mater.* **2017**, *132*, 578–590. [CrossRef]

24. Pan, X.; Shi, Z.; Shi, C.; Ling, T.C.; Li, N. A review on surface treatment for concrete–part 2: Performance. *Constr. Build. Mater.* **2017**, *133*, 81–90. [CrossRef]

25. Hou, P.K.; Kawashima, S.; Wang, K.J.; Corr, D.J.; Qian, J.S.; Shah, S.P. Effects of colloidal nanosilica on rheological and mechanical properties of fly ash-cement mortar. *Cement Concr. Compos.* **2013**, *35*, 12–22. [CrossRef]

26. Mei, J.; Tan, H.; Li, H.; Ma, B.; Liu, X.; Jiang, W.; Zhang, T.; Li, X. Effect of sodium sulfate and nano-SiO_2 on hydration and microstructure of cementitious materials containing high volume fly ash under steam curing. *Constr. Build. Mater.* **2018**, *163*, 812–825. [CrossRef]

27. Liu, M.; Tan, H.; He, X. Effects of nano-SiO_2 on early strength and microstructure of steam-cured high volume fly ash cement system. *Constr. Build. Mater.* **2019**, *194*, 350–359. [CrossRef]

28. Liu, X.; Ma, B.; Tan, H.; Zhang, T.; Mei, J.; Qi, H.; Chen, P.; Wang, J. Effects of colloidal nano-SiO_2 on the immobilization of chloride ions in cement-fly ash system. *Cem. Concr. Compos.* **2020**, *110*, 103596. [CrossRef]

29. Kumar, S.; Sirajudeen; Sivaranjani; Vani; Ali, N.; Begum, S.; Rahman, Z. Characterization, properties and microstructure studies of cement mortar incorporating nano-SiO_2. *Mater. Today Proc.* **2020**, in press. [CrossRef]

30. Wang, C.; Yang, H.; Chen, F.; Peng, L.; Gao, H.-F.; Zhao, L.-P. Influences of VTMS/SiO_2 ratios on the contact angle and morphology of modified super-hydrophobic silicon dioxide material by vinyl trimethoxy silane. *Results Phys.* **2018**, *10*, 891–902. [CrossRef]

31. Pantoja, M.; Abenojar, J.; Martinez, M.A. Influence of the type of solvent on the development of superhydrophobicity from silane-based solution containing nanoparticles. *Appl. Surf. Sci.* **2017**, *397*, 87–94. [CrossRef]

32. *UNI EN 1015-18:2004 Methods of Test for Mortar for Masonry-Determination of Water Absorption Coefficient Due to Capillary Action of Hardened Mortar*; Italian Standards: Milano, Italy, 2004.

33. Zhang, Y.; Li, S.; Zhang, W.; Chen, X.; Hou, D.; Zhao, T.; Li, X. Preparation and mechanism of graphene oxide/isobutyltriethoxysilane composite emulsion and its effects on waterproof performance of concrete. *Constr. Build. Mater.* **2019**, *208*, 343–349. [CrossRef]

34. *British Standard BS EN 14629:2007 Products and Systems for the Protection and Repair of Concrete Structures-Test Methods*; Determination of Chloride Content in Hardened Concrete; British Standards Institution: London, UK, 2007.

35. *ASTM C1202-97 Standard Test Method for Electrical Indication of Concrete's Ability to Resist Chloride Ion Penetration*; ASTM: West Conshohocken, PA, USA, 1997.

36. Cengiz, U.; Cansoy, C.E. Applicability of Cassie–Baxter equation for superhydrophobic fluoropolymer–silica composite films. *Appl. Surf. Sci.* **2015**, *335*, 99–106. [CrossRef]

37. Hou, P.; Kawashima, S.; Kong, D.; Corr, D.J.; Qian, J.; Shah, S.P. Modification effects of colloidal nanoSiO$_2$ on cement hydration and its gel property. *Compos. Part B* **2013**, *45*, 440–448. [CrossRef]

38. Ardalan, R.B.; Jamshidi, N.; Arabameri, H.; Joshaghani, A.; Mehrinejad, M.; Sharafi, P. Enhancing the permeability and abrasion resistance of concrete using colloidal nano-SiO$_2$ oxide and spraying nanosilicon practices. *Constr. Build. Mater.* **2017**, *146*, 128–135. [CrossRef]

39. Ren, J.; Lai, Y.; Gao, J. Exploring the influence of SiO$_2$ and TiO$_2$ nanoparticles on the mechanical properties of concrete. *Constr. Build. Mater.* **2018**, *175*, 277–285. [CrossRef]

40. Nazari, A.; Riahi, S. Microstructural, thermal, physical and mechanical behavior of the self compacting concrete containing SiO$_2$ nanoparticles. *Mater. Sci. Eng. A* **2010**, *527*, 7663–7672. [CrossRef]

41. Balapour, M.; Joshaghani, A.; Althoey, F. Nano-SiO$_2$ contribution to mechanical, durability, fresh and microstructural characteristics of concrete: A review. *Constr. Build. Mater.* **2018**, *181*, 27–41. [CrossRef]